Supplemental Materials

Processing of $CaLa_2S_4$ infrared transparent ceramics: a comparative study of HP and FAST/SPS techniques

Guillaume R. Durand, Quentin Bizot, Nathalie Herbert, Samuel Quéméré, Mathieu Pasturel, Xiang-Hua Zhang, Odile Merdrignac-Conanec

Univ Rennes, CNRS, ISCR (Institut des Sciences Chimiques de Rennes) - UMR 6226, F-35000 Rennes, France

Correspondence
Odile Merdrignac-Conanec, Institut des Sciences Chimiques de Rennes, UMR CNRS 6226, Equipe Verres et Céramiques, Université de Rennes1, Campus de Beaulieu, 35042 Rennes Cedex, France
Email : odile.merdrignac@univ-rennes1.fr

1. XRD characterization of as-combusted and sulfurized powders

Figures S1 (A) and S1 (B) show the XRD patterns of the as-combusted powder and sulfurized powder respectively. Pattern analysis of the as-combusted powder reveals the presence of lanthanum oxysulfate $La_2O_2SO_4$ (JCPDS 85-1535) and lanthanum oxide La_2O_3 (JCPDS 74-2430) as major phases and lanthanum oxysulfide La_2O_2S (JCPDS 71-2098) as minor phase. There is no evidence of CLS formation in the as-combusted powder, due to the oxidizing synthesis conditions. After heat-treatment at 1000°C for 4 h in H_2S, XRD patterns show pure CLS phase, without impurity or traces of secondary phases.

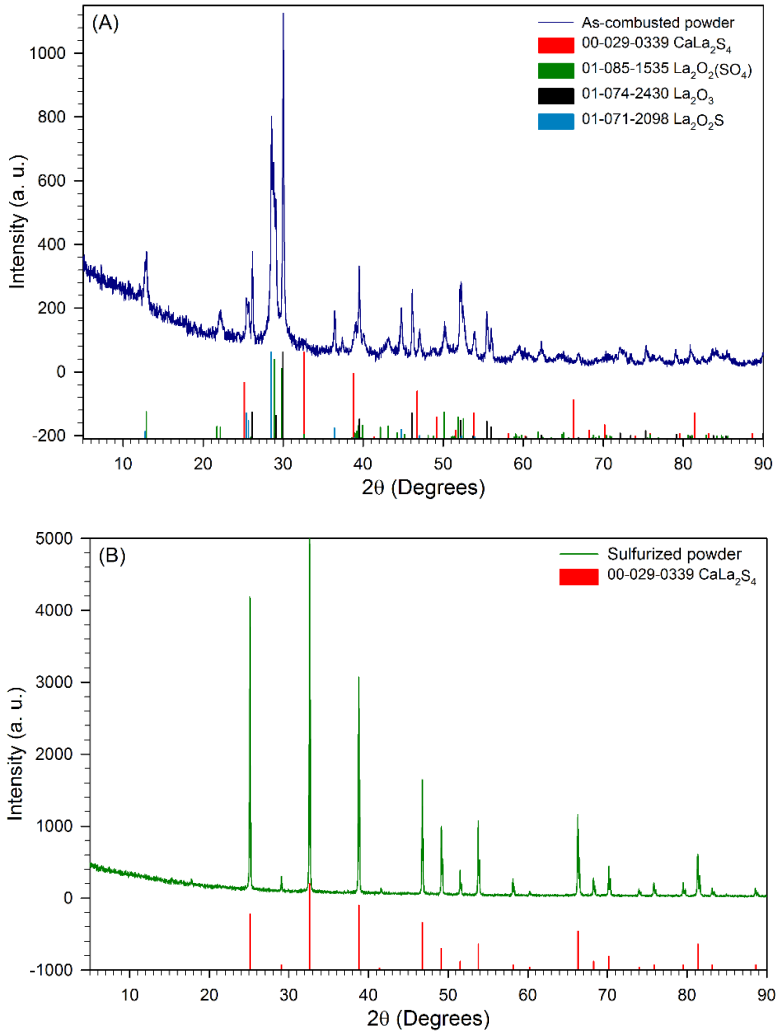

Figure S1: XRD patterns of powders (A) before (as-combusted) and (B) after treatment in H_2S at 1000 °C for 4 h (sulfurized)

2. FTIR characterization of as-combusted and sulfurized powders

Representative FTIR spectra of the as-combusted and sulfurized powders are shown in Figure S2. Powders were first diluted as 0.5% (weight) into FTIR grade KBr and pelletized in a stainless steel die (diam. = 13mm) under an uniaxial pressure of 5 tons. As-combusted powders show multiple absorption bands at 3300-3700 cm^{-1} and 1630 cm^{-1}, that are respectively characteristics of ν_3 asymmetric and ν_1 symmetric stretching and bending modes of the H_2O molecules[1–3]. The stretching vibrations, observed at 560-700 cm^{-1}, are attributed to the S-O vibration bands of $La_2O_2SO_4$ and La_2O_2S [4] previously identified by XRD. Finally, a large band can be observed around 1350-1580 cm^{-1} due to carbonate species[5, 6]. The latter is due to physi/chemi-sorbed CO_2 from the air and/or combustion. All the characteristic absorption bands observed in the as-combusted powder are removed by the sulfurization.

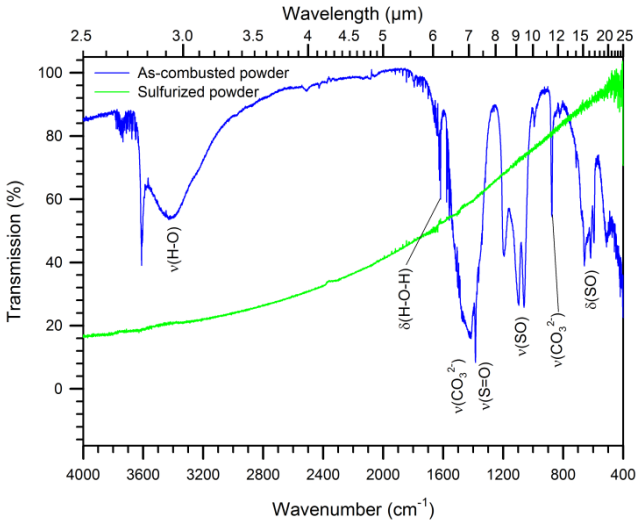

Figure S2: KBr-FTIR spectra of powders (A) before (as-combusted) and (B) after treatment in H_2S at 1000 °C for 4 h (sulfurized)

References

1. Janca A, Tereszchuk K, Bernath PF, *et al.* Emission spectrum of hot HDO below 4000 cm^{-1}. *J Mol Spectrosc*. 2003;219(1):132–135. https://doi.org/10.1016/S0022-2852(03)00015-8

2. Lemus R. Vibrational excitations in H_2O in the framework of a local model. *J Mol Spectrosc*. 2004;225(1):73–92. https://doi.org/10.1016/j.jms.2004.02.015

3. Panayotov DA, Yates Jr. JT. Depletion of conduction band electrons in TiO_2 by water chemisorption – IR spectroscopic studies of the independence of Ti–OH frequencies on electron concentration. *Chem Phys Lett*. 2005;410(1–3):11–17. https://doi.org/10.1016/j.cplett.2005.03.146

4. Richard A. Nyquist, Ronald O.Kagel. Handbook of Infrared and Raman Spectra of Inorganic Compounds and Organic Salts. 1971

5. Colthup N, Daly L, Wiberley S. Introduction to Infrared and Raman Spectroscopy - 3rd Edition. Academic Press. 1990

6. Capobianco JA, Vetrone F, D'Alesio T, Tessari G, Speghini A, Bettinelli M. Optical spectroscopy of nanocrystalline cubic $Y_2O_3:Er^{3+}$ obtained by combustion synthesis. *Phys Chem Chem Phys*. 2000;2(14):3203–3207. https://doi.org/10.1039/B003031G

3. Particle-size analysis of CLS powders

Figure S3 shows the particle size distribution of the sulfurized powders. CLS powders show a multi-modal broad particle size distribution, ranging from 0.05 µm to 30 µm. In consistency with SEM observations, three main populations can be identified which correspond to agglomerates with size centered on 15µm and 3-5µm composed of primary particles of size centered on 0.2-0.5 µm. Powders are characterized by particles/agglomerates size population of 0.4µm/6µm/14µm (d10/d50/d90).

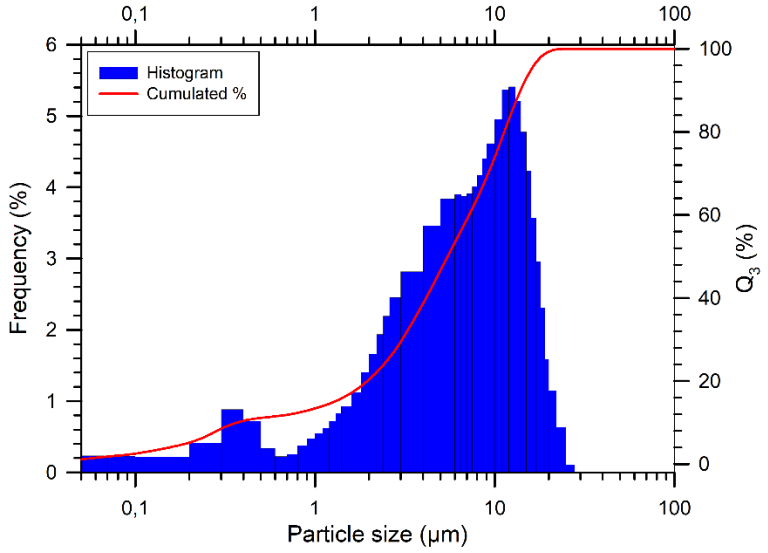

Figure S3: Particle size and cumulative size distribution of CLS powders

4. XRD patterns of ceramics Sintered by FAST

Figure S4 shows the XRD patterns of ceramics sintered by FAST. For each specimen, some fragments were manually crushed into a powder, because the Bragg-Bretano (θ-θ) geometry of the equipment does not allow the analysis of bulk sample as small as the fragments obtained by FAST sintering. All diffraction patterns are similar to the diffraction patterns of the powder and the ceramics sintered by HP.

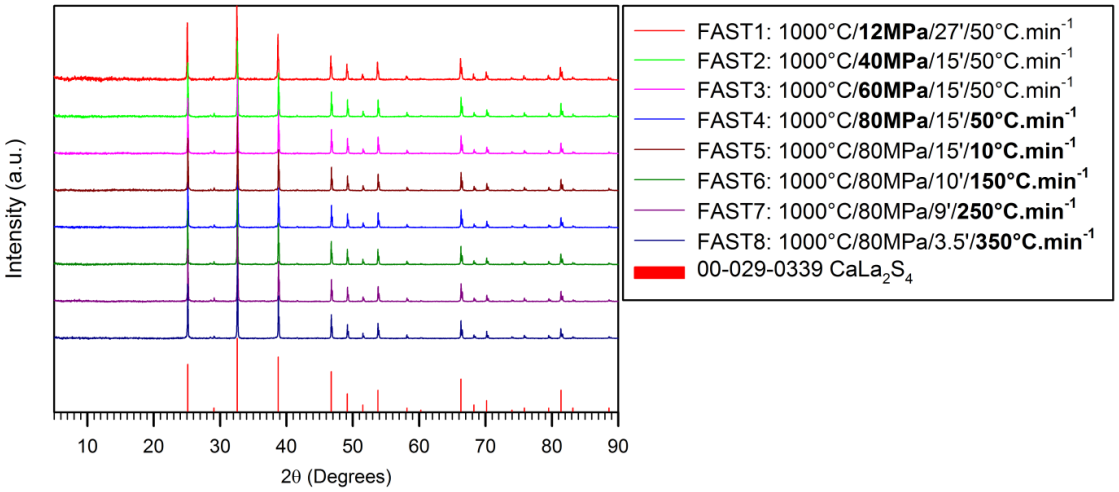

Figure S4: XRD patterns of FAST sintered ceramics

5. Micro-cracks of ceramics sintered by FAST

Figure S5 shows some representative examples of macro and micro-cracks observed on the ceramics sintered by FAST. These cracks seem to spread through the residual porosity, which is consistent to propagation mechanism through area with locally lower mechanical strength. These types of cracks are systematic for all the ceramics sintered by FAST.

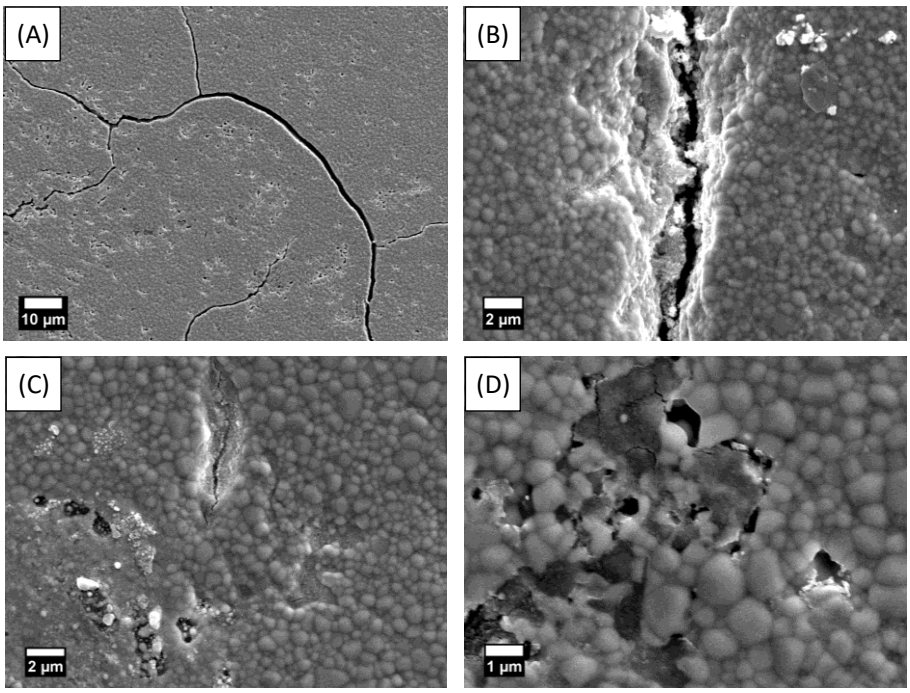

Figure S5: SEM micrographs of macro and micro-cracks of ceramics sintered by FAST. Examples of fractures observed respectively for (A) FAST2-40MPa (B) FAST4-80MPa (C) FAST5-10°C.min^{-1} (D) FAST8-350°C.min^{-1}